

Orientation of Functional and Nonfunctional PTS Permease Signal Sequences in Lipid Bilayers. A Polarized Attenuated Total Reflection Infrared Study^{†,‡}

Lukas K. Tamm* and Suren A. Tatulian

Department of Molecular Physiology and Biological Physics, University of Virginia, Health Sciences Center, Box 449, Charlottesville, Virginia 22908

Received December 18, 1992; Revised Manuscript Received April 16, 1993

ABSTRACT: Synthetic peptides corresponding to the N-terminal 23 and 22 residues, respectively, of two integral plasma membrane proteins of *Escherichia coli*, namely the mannitol- and glucitol-specific permeases of the bacterial sugar phosphotransferase system, were incorporated into single planar phospholipid bilayers supported on germanium plates. Polarized attenuated total reflection infrared spectra were recorded, and order parameters were derived from the measured dichroic ratios. The order parameters of the two wild-type peptides which form amphiphilic α -helices in membranes were -0.4 to -0.5 , indicating a preferential alignment of the α -helix long axis parallel to the membrane surface. Nonfunctional mutant peptides of the mannitol permease sequence in which serine-3 or aspartate-4 were substituted with prolines (S3P and D4P) or lysine (D4K), but which were still largely α -helical, exhibited peptide order parameters close to zero, indicating a high degree of disorder of these peptides in the lipid bilayers. The lipid was well ordered at low concentrations of peptides in the membranes but became disordered at high peptide concentrations. This effect of lipid disordering was more pronounced for the D4K mutant than for the wild-type mannitol peptide.

Most membrane proteins and most proteins that are transported across membranes are synthesized with N-terminal signal sequences which may or may not be proteolytically removed by a signal peptidase after membrane insertion. The signal peptides appear to have at least three functions (von Heijne, 1988; Gierasch, 1989; Tamm, 1991): (i) They direct proteins to the correct target membrane within the cell; (ii) they assist in the insertion of proteins into membranes; and (iii) they help prevent premature folding of proteins before they reach the membrane surface. Although quite a lot is known about the targeting function of several classes of signal sequences, our current knowledge of how the signal peptides actually insert into the membrane and how they facilitate the insertion and folding of the rest of the polypeptide chain in the membrane is much less well-understood. The bacterial phosphoenol pyruvate-dependent PTS¹ sugar permeases present an interesting case for studying this process because they have uncleaved signal sequences (Saier et al., 1988; Yamada et al., 1991) which structurally resemble the mitochondrial presequences. The PTS sugar permeases are integral membrane proteins of the cytoplasmic membranes of bacteria and are part of a larger enzyme complex which catalyzes the specific and energy-dependent uptake and phosphorylation of sugars from the environment (Saier, 1985). Both the mitochondrial presequences and the PTS permease

signal sequences adopt laterally amphiphilic α -helical conformations in membranes (Roise & Schatz, 1988; Tamm, 1991). This secondary structure motif is quite different from that of normal prokaryotic signal sequences which form longitudinally amphiphilic α -helices in lipid bilayer model membranes [for examples, see Gierasch (1989) and Batenburg et al. (1988)].

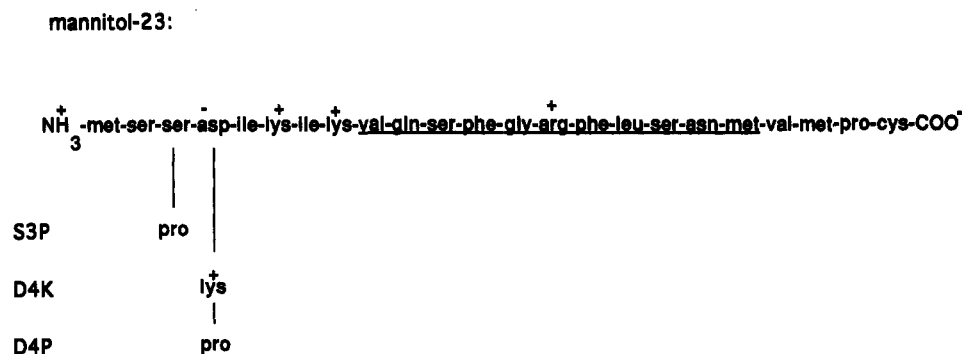
We have previously studied the interactions of two different PTS permease signal sequences with lipid model membranes (Tamm et al., 1989; Portlock et al., 1992). The chemically synthesized N-terminal peptides of the mannitol (23 residues) and the glucitol (22 residues) permeases were shown to form laterally amphiphilic α -helices when they were inserted into lipid bilayers or detergent micelles. The helical contents were rather high and ranged from 60 to 80%, depending on the particular sequence and the lipid environment. These peptides also exhibited high affinities for uncharged lipid bilayers, i.e., partition constants of 10^4 – 10^5 M⁻¹ were measured in monolayer and bilayer model systems. Recently, Yamada et al. (1991) identified five nonconservative single site mutations in positions 3 and 4 of the mannitol permease signal sequence which virtually abolished the correct insertion of the full length mannitol permease into the cytoplasmic membrane of *E. coli*. Since proteinaceous receptors for the PTS permease signal sequences are not known, we wanted to know whether these mutations had any effect on the physical interactions with membrane lipids. As a first step to identify differences in lipid-protein interactions between wild-type and mutant peptides, three variant peptides of the mannitol permease signal sequence which included the mutations serine 3 \rightarrow proline (S3P), aspartate 4 \rightarrow proline (D4P), and aspartate 4 \rightarrow lysine (D4K) were synthesized and compared with the wild-type peptide (Portlock et al., 1992). Their sequences are shown in Figure 1. These variant peptides were found to have the same secondary structure in lipid bilayers as the wild-type peptide and exhibited partition coefficients which were decreased maximally by a factor of 4 relative to the wild-type peptide. Clearly, differences in the secondary structures or

[†] This work was supported by grants from the Life and Health Insurance Medical Research Fund and the National Institutes of Health (R01-AI30557).

[‡] Dedicated to Prof. Harden M. McConnell on the occasion of his 65th birthday.

* Tel.: (804) 982-3578; FAX: (804) 982-1616; e-mail: 1kt2e@Virginia.EDU.

¹ Abbreviations: CD, circular dichroism; POPC, 1-palmitoyl-2-oleoyl-3-sn-phosphatidylcholine; POPG, 1-palmitoyl-2-oleoyl-3-sn-phosphatidylglycerol; PTS, phosphotransferase system; SPB, supported planar bilayer; SUV, small unilamellar vesicle; TFE, 2,2,2-trifluoroethanol; ATR, attenuated total reflection; IR, infrared; FTIR, Fourier transform infrared; mtl-23, 23 residue signal peptide of the mannitol PTS permease; gut-22, 22 residue signal peptide of the glucitol PTS permease.



glucitol-22:



FIGURE 1: Sequences of the synthetic mannitol and glucitol PTS permease signal peptides used in this work. Three single site mutations (S3P, D4P, and D4K) of the mannitol-23 sequence are also shown. The charges are as indicated, and the 11-residue segments with the largest hydrophobic moment (Eisenberg et al., 1984) are underlined.

the hydrophobic binding energies of these sequences could not explain the large functional differences that were found between the wild-type and mutant proteins *in vivo*. Another important physical parameter which could potentially discriminate between functional and nonfunctional signal peptides is the orientation of the α -helix in the membrane. A useful method for determining the orientation of α -helices in membranes is polarized attenuated total reflection infrared (ATR-IR) spectroscopy [for reviews, see Fringeli and Günthard (1981) and Goormaghtigh and Ruyschaert (1990)] on fully hydrated single supported planar bilayers (Frey & Tamm, 1991). In the present work, we have used this technique to measure the order parameters of the wild-type mannitol and glucitol permease signal peptides as well as those of the mutant peptides S3P, D4P, and D4K. The orientation of both wild-type peptides in lipid bilayers was predominantly parallel to the membrane surface, whereas the mutant peptides exhibited a high degree of orientational disorder in these model membranes. Also, one of the mutants (D4K) was much more effective than the wild-type peptide in disturbing the orientational order of the surrounding membrane lipids.

MATERIALS AND METHODS

Materials. POPC and POPG were purchased from Avanti Polar Lipids, Inc. (Alabaster, AL) and used without further purification. The peptides were synthesized by solid-phase methods and purified by reverse-phase high-performance liquid chromatography as described previously (Portlock et al., 1992). All other chemicals were from Sigma (St. Louis, MO), Fisher (Fair Lawn, NJ), or Eastman Kodak (Rochester, NY) and were of the highest available purity.

Vesicle Preparation. To prepare small unilamellar vesicles (SUV), 0.4 μmol of POPC and 0.1 μmol of POPG were mixed in chloroform. For experiments with peptides, an appropriate volume of peptide dissolved in TFE was added to the mixture of phospholipids in order to obtain the desired peptide-to-lipid ratio. The solvent was evaporated under a stream of nitrogen, 0.5 mL of phosphate buffered saline (10 mM NaP_i , 150 mM NaCl , pH 7.3) was added, and the liposomes were suspended by vigorous vortexing for 4–5 min. In some

experiments, the dried lipid-peptide mixtures were subjected to a high vacuum for 2 h to remove remaining trace amounts of solvent before they were hydrated with buffer. No significant differences were observed between the CD or IR spectra of these and the nonevacuated samples. The suspension was then subjected to five cycles of freezing and thawing using liquid nitrogen and hot water, followed by 15 cycles of extrusion through two 100-nm pore size polycarbonate membranes (Nucleopore, Pleasanton, CA) using the syringe-type Liposofast extruder (Avestin, Ottawa, Canada) (MacDonald et al., 1991).

Preparation of Supported Bilayers. Planar phospholipid bilayers supported on germanium ATR-IR plates were prepared as previously described (Frey & Tamm, 1991; Kalb et al., 1992). Briefly, a monomolecular film of POPC was formed on the surface of an aqueous buffer (10 mM Tris-acetic acid, 0.002% NaN_3 , pH 5.0) in a circular Fromherz trough (Mayer, Göttingen, Germany) by spreading a 1.5 mM lipid solution in a 9:1 (v/v) hexane/ethanol mixture on the air-water interface at zero surface pressure and allowing 10 min for solvent evaporation. The monolayer was slowly compressed to a surface pressure of 32 mN/m which was maintained constant during the subsequent Langmuir-Blodgett deposition by adjusting the surface area of the monolayer with an electronic feedback circuit. The germanium plate (50 \times 20 \times 1 mm³ with 45° beveled edges; Buck Scientific, Norwalk, CT) was cleaned with chloroform/methanol, followed by 10 min argon plasma cleaning (Harrick, Ossining, NY), immersed vertically through the monolayer, and withdrawn at a lower speed (approximately 4 mm/min). No significant change in the surface area was detected during immersion of the plate, whereas the decrease in the surface area during withdrawal was roughly equal to the total substrate surface area. The plate was assembled in between two identical halves of the measuring cell which had an internal volume of 0.5 mL. The suspension of SUV was injected into the cell so that both sides of the germanium plate were exposed to the vesicles. The cell was gently shaken on Hoefer rotor (Hoefer Scientific Instruments, San Francisco, CA) for 30 min to allow the vesicles to fuse with the monolayer and to yield a

supported phospholipid bilayer with or without peptide. To remove unfused vesicles and to replace H_2O by D_2O , the cell was flushed with 6 mL of H_2O followed by 6 mL of D_2O .

Infrared Spectroscopy. Infrared spectra were recorded on a Nicolet 740 Fourier-transform infrared spectrometer (Nicolet Analytical Instruments, Madison, WI) equipped with an ATR-IR accessory (Buck Scientific, Norwalk, CT). The infrared beam was polarized with a goldwire grid polarizer (Perkin-Elmer, Beaconfield, U.K.) and allowed to enter the germanium plate normal to the 45° beveled edge. Under these conditions, the infrared beam travels along the plate by undergoing about 35 total internal reflections before it exits the plate and is directed to the liquid-nitrogen-cooled mercury-cadmium-telluride detector. In a typical protocol, parallel and perpendicular polarized attenuated total reflection infrared spectra in the range $400\text{--}4400\text{ cm}^{-1}$ were measured on the bare germanium plate in contact with D_2O ; 2000 scans were collected at each polarization with a resolution of 2 cm^{-1} . Polarized spectra were then recorded under identical conditions on the germanium plate with the supported bilayer. The corresponding spectra with and without bilayer were ratioed and converted to absorbance spectra at each polarization. The dichroic ratios were calculated for the bands of interest by dividing the absorbance at the respective peak maxima ($R^{\text{ATR}} = A_{\parallel}/A_{\perp}$). Since these bands were all well resolved, band deconvolution was not necessary, and R^{ATR} ratios calculated from integrated bands gave essentially the same results as those deduced from the peak heights. The measured R^{ATR} values were used to evaluate the order parameters of the lipids and peptides.

Determination of the Peptide and Lipid Order Parameters. For an axially symmetric molecule which fluctuates around the z axis (i.e., the normal to the surface of the supported bilayer membrane), an order parameter S can be defined which is a function of the amplitudes of the time- and space-averaged fluctuations around z as measured by the excursion angle θ :

$$S = (3\langle \cos^2 \theta \rangle - 1)/2 \quad (1)$$

The order parameter of the α -helical part of a peptide in a supported phospholipid bilayer can be derived from the measured dichroic ratio of the amide I band at around 1642 cm^{-1} by using the expression (Frey & Tamm, 1991)

$$S = 2B/[f(3\cos^2 \alpha - 1)(B - 3E_z^2)] \quad (2)$$

where $B = E_x^2 - R^{\text{ATR}}E_y^2 + E_z^2$. E_x , E_y , and E_z are the components of the electric field of the evanescent wave at the germanium-buffer interface (Frey & Tamm, 1991). They are functions of the angle of incidence of the IR beam at the germanium-buffer interface and of the refractive indices of the substrate (Ge), the phospholipid bilayer, and the ambient phase (D_2O). In the present work, we have used refractive indices of 4.0 for germanium, 1.43 for the phospholipid bilayer, and 1.33 for D_2O (Wolfe & Zissis, 1978; Fringeli et al., 1989). Using the thin film approximation (Harrick, 1967; Frey & Tamm, 1991), E_x^2 , E_y^2 , and E_z^2 become 1.9691, 2.2486, and 1.8917, respectively. In eq 2, f is the fraction of amino acid residues in α -helical conformation, and α is the angle of the orientation of the transition moment of the vibration relative to the molecular director. A value of $\alpha = 39^\circ$ was used for the mean orientation of the transition moment of the amide I vibration with respect to the long axis of the α -helix (Tsuboi, 1962; Bradbury et al., 1962). The fractions of residues in α -helical conformation were used as estimated earlier from circular dichroism spectroscopy for each of the peptides in POPG or POPC bilayers, namely, $f = 0.63, 0.76, 0.82, 0.77$,

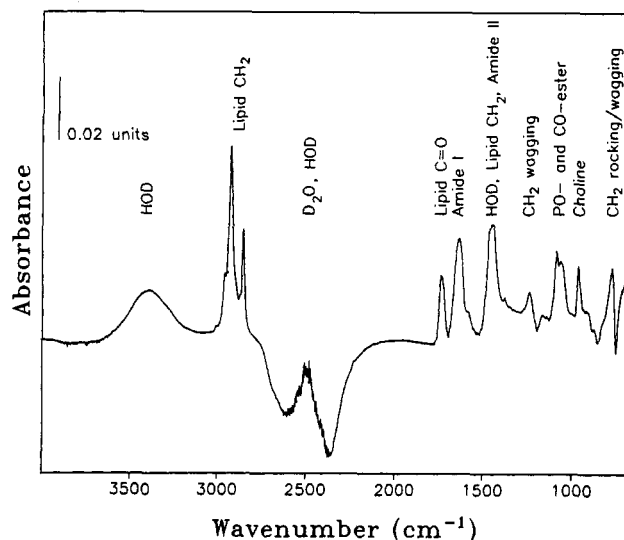


FIGURE 2: Perpendicular polarized ATR-IR spectrum of a single planar bilayer of POPC/POPC:POPG (4:1) with incorporated mtl-23 peptide supported on a flat germanium substrate. The nominal peptide-to-lipid molar ratio was 1:30. Several prominent bands are assigned. The sample was prepared in H_2O and then exchanged with D_2O . An incomplete isotope exchange explains the residual HOD bands. For the geometric arrangement and definitions of coordinates, see Figure 1 in Frey and Tamm (1991).

and 0.54 for mtl-23, S3P, D4P, D4K, and gut-22, respectively (Portlock et al., 1992).

The general eq 2 may also be used to calculate the order parameters of the phospholipids in the supported bilayers from the intensities of the symmetric and antisymmetric CH_2 stretching vibrations at 2853 and 2923 cm^{-1} , respectively. Since the transition moments of these vibrations are oriented perpendicular to the long axis of all-trans hydrocarbon chains, and since all methylene segments in the system contribute to the measured signals, values of $\alpha = 90^\circ$ and $f = 1$ are inserted and eq 2 reduces to

$$S_L = 2B/(3E_z^2 - B) \quad (3)$$

Since the dispersion between 1600 and 3000 cm^{-1} is rather small (Wolfe & Zissis, 1978), the same optical constants E_x^2 , E_y^2 , and E_z^2 , were used for calculating the lipid and peptide order parameters.

RESULTS

Asymmetric supported planar bilayers (SPBs) were formed on germanium ATR-IR plates. These bilayers were composed of a pure POPC leaflet facing the substrate and a second POPC/POPG (4:1) leaflet facing the bulk aqueous phase. Difference ATR-FTIR spectra (Ge/bilayer/ D_2O -Ge/ D_2O) were recorded with parallel and perpendicular polarized light in the range from 400 to 4400 cm^{-1} . An overview of a characteristic IR absorbance spectrum of a single planar phospholipid bilayer with the 23-residue wild-type mannitol permease signal peptide (mtl-23) is presented in Figure 2. This bilayer was formed by incubating the supported monolayer with vesicles that were prepared at a nominal² peptide-to-lipid molar ratio of 1:30. The actual peptide-to-lipid ratio in the supported bilayer was then estimated from the integrated amide I and methylene stretching vibrations at $1600\text{--}1690$ and $2800\text{--}2980\text{ cm}^{-1}$, respectively. Since we are dealing with oriented molecules in a polarized evanescent wave, Beer-

² The nominal peptide-to-lipid ratio is the input ratio that was used to make the extruded vesicles.

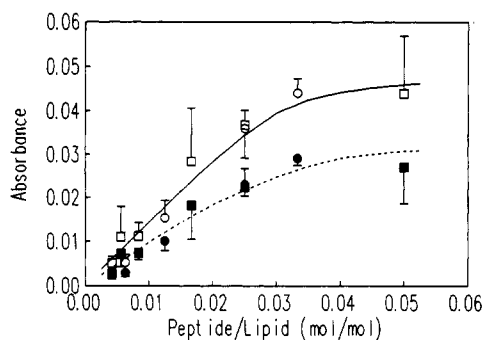


FIGURE 3: Change of the amide I band intensity as a function of the nominal peptide-to-lipid molar ratio. The intensities for the mtl-23 (●, ○) and for the mtl-23(D4K) (■, □) peptides are calculated from the parallel polarized (open symbols) and perpendicular polarized (closed symbols) IR spectra. The incorporation of the peptides into lipid bilayers approaches saturation at a nominal peptide-to-lipid molar ratio of about 1:30.

Lambert's law does not apply in its usual simple form, but equivalent expressions can be derived for parallel and perpendicular polarized light (see Appendix). Using eq A4, we determined the actual peptide-to-lipid molar ratio in the supported bilayer from the measured integrated peptide and lipid bands of Figure 2 to be approximately 1:15. Many other spectra of all five peptides of this study and at many different peptide-to-lipid ratios were analyzed by this same procedure. The actual peptide-to-lipid ratios were always found to be approximately twice as large as the nominal input ratios. The ratio between the actual and nominal peptide-to-lipid ratios did not change from nominal 1:120 to 1:30 and averaged at 2.0 ± 0.4 . Evidence for a linear relationship between the input concentrations and the resulting peptide concentrations in the supported bilayer is presented in Figure 3. The peak absorbances of the amide I bands are a linear function of the input ratios and saturate only at nominal peptide-to-lipid ratios greater than 1:30. Therefore, all subsequent spectra that were used for order parameter determinations were recorded at actual peptide-to-lipid ratios of 1:15 or lower and only actual ratios which were calculated by multiplying the nominal ratios by 2 are reported in the following paragraphs.

Orientation of the Phospholipids in Supported Planar Bilayers. The spectral regions that include the lipid CH_2 stretching vibrations are presented in Figure 4 for a planar lipid bilayer in the absence of peptide (Figure 4A) and in the presence of the mtl-23 mutant peptide (D4K) which was incorporated at a peptide-to-lipid molar ratio of 1:20 (Figure 4B). Of all the peptides used in this study, the mtl-23(D4K) had the most pronounced effect on the lipid order. The dichroic ratios derived from the CH_2 stretching vibrations of the lipid acyl chains were 1.29 in the absence of peptide and 1.69 in the presence of mtl-23(D4K) at a 1:20 molar ratio. (For a given membrane the values of R^{ATR} calculated from the symmetric and antisymmetric CH_2 stretching vibrations were the same with an accuracy of 1–5%.) By using eq 3, lipid order parameters of 0.41 and 0.02 were calculated from the dichroic ratios without and with the peptide, respectively. The lipid order parameter in the absence of peptide was close to that previously observed (Frey & Tamm, 1991) and is consistent with a well-ordered lipid film (parallel to the plane of the germanium plate) in which the methylene groups have segmental flexibility and are disordered to a degree which is typical for a lipid bilayer in the liquid-crystalline phase. The strongly decreased order parameter in the presence of 5 mol % of mtl-23(D4K) implies that this peptide can disturb the orientational order of the lipid molecules to a large degree.

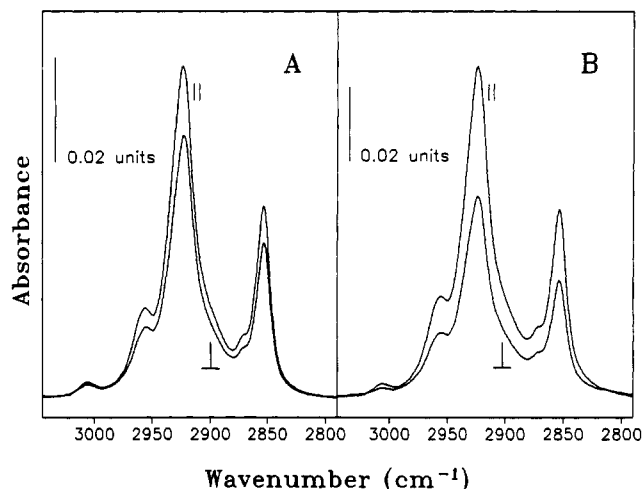


FIGURE 4: Polarized ATR-IR spectra of the methylene stretching region of the lipids in single planar bilayers supported on germanium: (A) POPC/POPC:POPG (4:1) bilayer without peptide and (B) POPC/POPC:POPG (4:1) bilayer with the mutant peptide mtl-23(D4K) at a peptide-to-lipid molar ratio of 1:20. Note the different dichroic ratios of 1.265 and 1.656 in A and B, respectively. The peaks at 2923 and 2853 cm^{-1} represent the antisymmetric and symmetric lipid methylene stretch vibrations, respectively.

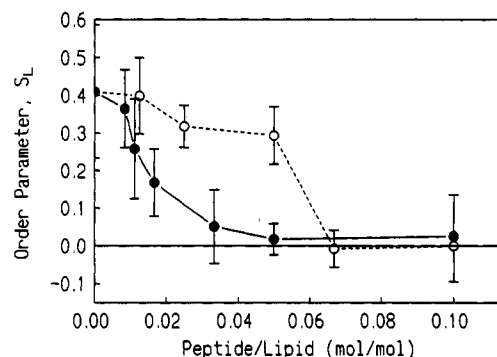


FIGURE 5: Order parameters of the lipid hydrocarbon chains as a function of the peptide-to-lipid ratio in supported bilayers. The mutant peptide mtl-23 (D4K) (●) is more effective than the wild-type peptide mtl-23 (○) in disordering the lipid bilayer.

Whether this disordering is at the level of segmental chain flexibility (trans-gauche isomerizations) or whether it affects the orientation of the entire lipid molecules cannot be decided with the present experiments.

The effect on the lipid order is not the same for all the peptides that have been measured in this work. The data presented in Figure 5 demonstrate that an increase of the mtl-23(D4K)/lipid molar ratio to 1:30 decreases the lipid order parameter dramatically. In contrast, the wild-type mtl-23 peptide has a much smaller effect on the lipid order parameter than the D4K mutant. Good lipid order is maintained with this peptide up to a peptide-to-lipid molar ratio of 1:20.

Orientation of the Peptides in Supported Planar Bilayers. Having determined the order parameters of the lipid molecules at various peptide-to-lipid molar ratios and for the different peptides of this study, the order parameters of the helical peptides were measured in the same SPB preparations. The peptide order parameters were only evaluated when the lipids were well ordered, i.e., when the lipid order parameters in the same preparations were 0.25 or higher. Figure 6 shows polarized ATR-IR spectra in the 1500–1800- cm^{-1} region which includes the carbonyl stretching vibrations of the lipids and the amide I band of the peptides. The spectra of the wild-type

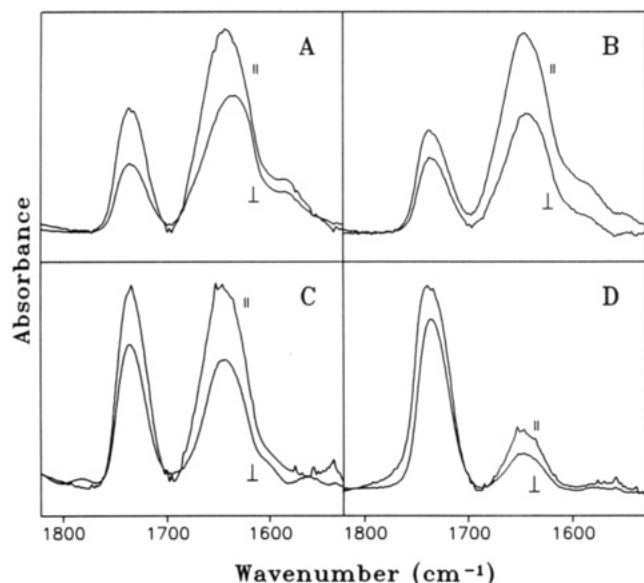


FIGURE 6: Polarized ATR-IR spectra of the amide I region of various peptides incorporated into single planar bilayers supported on germanium: (A) mtl-23 in POPC/POPC:POPG (4:1) at a peptide-to-lipid molar ratio of 1:20, (B) mtl-23(S3P) in POPC/POPC:POPG (4:1) at a peptide-to-lipid molar ratio of 1:30, (C) mtl-23(D4P) in POPC/POPC:POPG (4:1) at a peptide-to-lipid molar ratio of 1:20, and (D) mtl-23(D4K) in POPC/POPC:POPG (4:1) at a peptide-to-lipid molar ratio of 1:60. The ATR dichroic ratios of the amide I bands at about 1642 cm^{-1} are 1.48, 1.67, 1.59, and 1.66 in panels A, B, C, and D, respectively. The bands at 1735 cm^{-1} are assigned to the lipid carbonyl ester stretch vibrations.

mtl-23 peptide (panel A) and of the S3P and D4P mutant peptides (panels B and C, respectively) were recorded at peptide-to-lipid ratios of 1:20 or 1:30, but the peptide-to-lipid ratio in the case of D4K (panel D) was 1:60. It was necessary to compare the dichroic ratios of the D4K mutant at this lower peptide-to-lipid molar ratio because of the stronger disordering effect of this peptide on the surrounding lipids (see above). The dichroic ratios of the amide I bands were determined from the spectra shown in Figure 6, and the corresponding peptide order parameters as calculated by eq 2 were -0.41 , -0.07 , -0.16 , and -0.08 for the wild-type mtl-23 and the S3P, D4P, and D4K mutant peptides, respectively.

For each peptide and at each peptide-to-lipid ratio, the order parameters were measured in three to eight independent experiments. The average order parameters from these experiments and the corresponding standard deviations are graphically summarized in Figure 7. It is evident from Figure 7 that the two wild-type peptides, gut-22 and mtl-23, exhibit order parameters which are close to the theoretical limit of -0.5 . This limit is expected for an α -helix that is perfectly aligned parallel to the plane of the membrane ($\theta = 90^\circ$ in eq 1). Therefore, the average orientation of gut-22 and mtl-23 must be close to parallel to the membrane surface. In contrast, all three mutant peptides (S3P, D4P, D4K) show much lower order parameters. In fact, their order parameters are quite close to zero which implies a random orientation of these peptides in the lipid bilayer. (Alternatively, an orientational distribution around the "magic" angle of 54.7° or some other combination of angles could also yield $S = 0$; see eq 1.) Clearly, the orientational distributions of the three mutant peptides are distinctly different from the orientations of the two wild-type peptides which are coplanar with the membrane surface.

DISCUSSION

The most significant result of the present work is that compared to the wild-type signal peptides, some single site

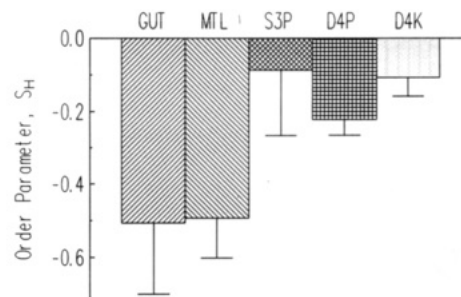


FIGURE 7: Order parameters of the helical regions of five different peptides in single planar bilayers supported on germanium. The order parameters of the two wild-type peptides, gut-22 and mtl-23, are near -0.5 , which is the theoretical limit for a perfect alignment parallel to the membrane surface. The order parameters of the three mutant peptides are much closer to zero, which is expected for a more random orientation of the peptides in the membrane. The data compiled for this plot include averages of three to eight independent measurements for each peptide.

mutations of the mannitol PTS permease signal peptide of *E. coli* change the orientation of their amphiphilic α -helices relative to the lipids in the bilayer and that these changes strictly correlate with the membrane targeting function of the corresponding signal sequences *in vivo* [cf. Yamada et al. (1991)]. The assignment of an orientation of the wild-type signal peptides of the glucitol and mannitol PTS permeases close to parallel to the plane of the membrane is unambiguous. The measured order parameters are near the theoretical limit of -0.5 for a rigid alignment of the α -helical part of the peptides parallel to the membrane surface. This orientation is not surprising in view of the strong helical hydrophobic moment that has been found between residues 2 and 18 for the glucitol signal peptide and between 8 and 21 for the mannitol signal peptide, respectively [Tamm, 1991; see also Figure 7 of Portlock et al. (1992)]. The changes in orientation of the single site mutant peptides of the mannitol PTS permease signal sequence are more difficult to explain. The experimental order parameters which range between 0 and -0.2 for the three mutant peptides cannot be unambiguously assigned to a fixed angle (θ) or even to a single angular distribution relative to the lipid bilayer. Nevertheless and irrespective of the actual orientational distribution, the order parameters of the mutant peptides are significantly different from those of the wild-type peptides and are not coplanar with the bilayer surface. They may be more obliquely inserted into the bilayer or orientationally more randomized. A single order parameter cannot decide between these two possibilities (or combinations of the two).

The amide I bands of the membrane-bound peptides in D_2O are all centered at around 1642 cm^{-1} . This value is about 10–12 wave numbers lower than the amide I band that is usually observed for α -helices with amide protons (Susi and Byler, 1986). However, an isotope shift is known to occur in α -helices in which the amide protons have been exchanged with deuterons. The position of the amide I band of a fully deuterium exchanged α -helix may be as low as 1635 cm^{-1} (Susi et al., 1967). Since the PTS permease signal peptides are known from CD spectroscopy to be α -helical in membranes (Portlock et al., 1992), the positions of the amide I bands indicate that the isotope exchange of the amide protons was quite extensive.³ For a comparison, the helical, membrane

³ This conclusion is further supported by the fact that we observe very little absorbance at 1543 cm^{-1} , i.e., the expected position of the protonated amide II band. The deuterated amide II band is expected at 1460 cm^{-1} and overlaps with the HOD bending and lipid CH_2 scissoring modes.

surface-bound bee venom peptide melittin in D₂O had an amide I band centered at 1644 cm⁻¹ (Frey and Tamm, 1991), i.e., only slightly above the value reported here for the PTS permease signal peptides. However, recent measurements on a hydrophobic peptide that spans the lipid bilayer in a single α -helix showed an amide I band in D₂O at 1652 cm⁻¹, i.e., a position indicating that practically no amide proton exchange has occurred [Tatullian and Tamm, unpublished experiments; see also Zhang et al. (1992)]. An isotope exchange can only happen when the amide protons are accessible to water and when they are not hydrogen bonded in a stable secondary structure. Therefore, the surface-bound PTS permease peptides are likely to be in an equilibrium with a non-helical, soluble form. The partition constants of $(2-8) \times 10^4 \text{ M}^{-1}$ that have been measured earlier for the partitioning of these peptides between a monolayer of POPC and buffer (Portlock et al., 1992) are consistent with this idea.⁴

Quantitative estimates of the peptide-to-lipid ratios showed that the peptide concentrations in the supported bilayers are approximately twice as large as those in the vesicles from which they were derived. The following two mechanisms may explain the enrichment of peptide in the supported membranes: First, the vesicle population may not be uniform, and vesicles with a higher peptide concentration may have a greater probability for fusion with the supported monolayers. In vesicle systems, the rate of membrane fusion is known to be accelerated by several amphiphilic peptides (Parente et al., 1990; Epand et al., 1992; Murata et al., 1992; Yoshimura et al., 1992). Second, some peptide may be transferred directly from the vesicles to the supported membrane by a simple partition reaction without a simultaneous transfer of lipid.⁵

To the best of our knowledge, the present work represents the first report on a correlation between the orientation of signal sequences in lipid model membranes and their functionality *in vivo*. Correlations between the ability to form α -helices in membranes and signal sequence function have been found before for the longitudinally amphiphilic α -helix-forming signal peptides of the *lamB* receptor and the *phoE* porin of *E. coli* (McKnight et al., 1989; Batenburg et al., 1988). The question of signal peptide orientation in the bilayer was also addressed in an ATR-IR study on the *lamB* signal sequence (Cornell et al., 1989). The average orientation of this α -helix was parallel to the fatty acyl chains when the peptide was incorporated at a low monolayer surface pressure (22 mN/m), but the peptide was found to be in a β -strand conformation at a higher surface pressure (37 mN/m). Unfortunately, these experiments were carried out with adsorbed peptide-lipid monolayers in the absence of water. It is known, on the other hand, that the orientation of melittin and alamethicin in membranes can change quite dramatically when the degree of hydration is changed in the membrane preparations (Frey & Tamm, 1991; Huang & Wu, 1991).

What is the significance of the orientations of the wild-type and mutant PTS permease signal peptides in lipid bilayers?

⁴ Unfortunately, it is not feasible to follow the isotope exchange kinetics under our current experimental conditions because this exchange appears to be completed after about 1–2 h, i.e., the time that is needed to purge the sample compartment of the spectrometer before the first spectrum can be recorded.

⁵ The relatively strong amide I band cannot be due to an excess of free peptide in the evanescent wave. The evanescent wave penetrates 39 nm from the germanium surface into the solution under our experimental conditions. Simple calculations with the known partition constants of these peptides (Portlock et al., 1992) show that the contributions of the free peptides can only amount to about 0.025–0.1% of the total measured ATR-IR signal.

Since these peptides are not cleaved and, therefore, constitute part of the mature PTS permeases (Yamada et al., 1991), they may well be important for the correct folding of the entire polypeptide chain in the membrane. Whether or not accessory proteins, such as the *sec* gene products, are needed for the insertion of the PTS permeases into biological membranes is not presently known. It has been proposed (Portlock et al., 1992) that about 4–5 residues amphiphilic β -strand may be formed between residues 4–8, i.e., N-terminal to the proposed amphiphilic α -helix of the mannitol permease signal peptide. The introduction of prolines or a lysine in positions 3 and 4 may disrupt this feature which in turn may be needed for a proper orientation of the amphiphilic α -helix parallel to the bilayer surface. The proposed amphiphilic α -helix of the glucitol peptide is a few residues longer than that of the mannitol peptide and, therefore, may not require the help of an additional amphiphilic structural element for an orientation parallel to the surface of the membrane. Alternatively, the mutant peptides may more likely aggregate into oligomers than the wild-type peptides. The individual subunits in the oligomer may then each become oriented at a different angle in the bilayer, or the oligomer itself may not orient well in the membrane. One or both of these two mechanisms might also change the orientation of the N-terminal α -helix of the full-length protein and could explain the incorrect membrane assembly of the mannitol permease *in vivo*.

ACKNOWLEDGMENT

We thank D. Mullins and S. Portlock for their valuable assistance in the early phases of this work.

APPENDIX: ESTIMATES OF LIPID-TO-PROTEIN RATIOS IN SUPPORTED PLANAR BILAYERS BY ATR-IR

The general equations of Beer–Lambert's law for integrated absorption bands in an oriented thin film using polarized total internal reflection illumination are (Harrick, 1967; Fraser & MacRae, 1973; Frey & Tamm, 1991)

$$\int A_{\parallel}(\tilde{\nu}) d\tilde{\nu} = \int \epsilon(\tilde{\nu}) d\tilde{\nu} c N \frac{n_{31}d}{\cos \gamma} \{E_x^2[(S \sin^2 \alpha)/2 + (1 - S)/3] + E_z^2[S \cos^2 \alpha + (1 - S)/3]\} \quad (\text{A1})$$

$$\int A_{\perp}(\tilde{\nu}) d\tilde{\nu} = \int \epsilon(\tilde{\nu}) d\tilde{\nu} c N \frac{n_{31}d}{\cos \gamma} E_y^2[(S \sin^2 \alpha)/2 + (1 - S)/3] \quad (\text{A2})$$

where $\int A_{\parallel, \perp}(\tilde{\nu}) d\tilde{\nu}$ are the integrated absorption bands measured with parallel and perpendicular polarized light, respectively, $\int \epsilon(\tilde{\nu}) d\tilde{\nu}$ is the integral molar absorption coefficient, c is the concentration of molecules or chemical groups giving rise to the absorption, N is the number of active total internal reflections, d is the thickness of the thin film, $n_{31} = n_3/n_1$ is the ratio of the refractive index of the buffer solution to the refractive index of the internal reflection element, γ is the angle of incidence of the IR beam on the reflecting interface, E_x , E_y , and E_z are the electric field components of the evanescent wave, S is the order parameter, and α is the angle of the transition moment to the molecular director axis.

It is seen from eq A1 and A2 that the ratios of two different bands are more easily compared in perpendicular polarized spectra, because in this case the electric field components which depend on the various refractive indices (including that of the thin film) cancel out. The ratio of the integrated

absorbances of two bands measured with perpendicular polarized light is

$$\frac{\int A_{\perp}(\tilde{\nu}_1) d\tilde{\nu}}{\int A_{\perp}(\tilde{\nu}_2) d\tilde{\nu}} = \frac{c_1 \sigma_1 \int \epsilon(\tilde{\nu}_1) d\tilde{\nu}}{c_2 \sigma_2 \int \epsilon(\tilde{\nu}_2) d\tilde{\nu}} \quad (\text{A3})$$

where $\sigma_i = (S_i \sin^2 \alpha_i)/2 + (1 - S_i)/3$. Therefore, knowing the integrated molar absorption coefficients, the order parameters, and the angles of the transition moments in the molecule, we can determine the lipid-to-protein ratio in supported bilayers from the integrated band intensities of the lipid methylene stretch and the amide I vibrations.

$$L/P = 0.208 (n_{\text{res}} - 1) (\sigma_2/\sigma_1) \frac{\int A_{\perp}(\tilde{\nu}_1) d\tilde{\nu}}{\int A_{\perp}(\tilde{\nu}_2) d\tilde{\nu}} \quad (\text{mol/mol}) \quad (\text{A4})$$

To arrive at the molar lipid-to-protein ratio in eq A4, the number of residues of the peptide (n_{res}) was introduced, and numerical values for the integrated molar absorption coefficients of the methylene stretching vibrations (1.32×10^8 cm/mol of lipid, integrated from 2800 to 2980 cm^{-1} ; Fringeli et al., 1989) and of the amide I vibration (2.74×10^7 cm/mol of peptide bond, integrated from 1600 to 1690 cm^{-1} ; Fringeli et al., 1989) were inserted. The indices 1 and 2 refer to the lipid and peptide bands, respectively.

REFERENCES

- Batenburg, A. M., Brasseur, R., Ruysschaert, J.-M., Scharrenburg, A. M., Slotbloom, A. J., Demel, R. A., & deKruijff, B. (1988) *J. Biol. Chem.* **263**, 4202–4207.
- Bradbury, E. M., Brown, L., Downie, A. R., Elliott, A., Fraser, R. D. B., & Hanby, W. E. (1962) *J. Mol. Biol.* **5**, 230–247.
- Cornell, D. G., Dluhy, R. A., Briggs, M. S., McKnight, C. J., & Gierasch, L. M. (1989) *Biochemistry* **28**, 2789–2797.
- Epand, R. M., Cheetham, J. J., Epand, R. F., Yeagle, P. L., Richardson, C. D., Rockwell, A., & DeGrado, W. F. (1992) *Biopolymers* **32**, 309–314.
- Fraser, R. D. B., & MacRae, T. P. (1973) *Conformation in Fibrous Proteins and Related Synthetic Peptides*, Academic Press, New York.
- Frey, S., & Tamm, L. K. (1991) *Biophys. J.* **60**, 922–930.
- Fringeli, U. P., & Günthard, H. H. (1981) In *Membrane Spectroscopy* (Grell, E., Ed.) Springer-Verlag, Berlin, pp 270–332.
- Fringeli, U. P., Apell, H. J., Fringeli, M., & Luger, P. (1989) *Biochim. Biophys. Acta* **984**, 301–312.
- Gierasch, L. M. (1989) *Biochemistry* **28**, 923–930.
- Goormaghtigh, E., & Ruysschaert, J.-M. (1990) In *Molecular Description of Biological Membranes by Computer-Aided Conformational Analysis* (Brasseur, R., Ed.) CRC Press, Boca Raton, FL, pp 285–329.
- Harrick, N. J. (1967) *Internal Reflection Spectroscopy*, Harrick Scientific Corporation, New York.
- Huang, H. W., & Wu, Y. (1991) *Biophys. J.* **60**, 1079–1087.
- Kalb, E., Frey, S., & Tamm, L. K. (1992) *Biochim. Biophys. Acta* **1103**, 307–316.
- McKnight, C. J., Briggs, M. S., & Gierasch, L. M. (1989) *J. Biol. Chem.* **264**, 17 293–17 297.
- Murata, M., Takahashi, S., Kagiwada, S., Suzuki, A., & Ohnishi, S. (1992) *Biochemistry* **31**, 1986–1992.
- Parente, R. A., Nadasdi, L., Subbarao, N. K., & Szoka, F. C., Jr. (1990) *Biochemistry* **29**, 8713–8719.
- Portlock, S. H., Lee, Y., Tomich, J., & Tamm, L. K. (1992) *J. Biol. Chem.* **267**, 11017–11022.
- Saier, M. H., Jr. (1985) *Mechanisms and Regulation of Carbohydrate Transport in Bacteria*, Academic Press, New York.
- Saier, M. H., Jr., Yamada, M., Erni, B., Suda, K., Lengeler, J., Ebner, R., Argos, P., Rak, B., Schnetz, K., Lee, C. A., Stewart, G. C., Breidt, F., Jr., Waygood, E. B., Peri, K. G., & Doolittle, R. F. (1988a) *FASEB J.* **2**, 199–208.
- Saier, M. H., Jr., Yamada, M., Suda, K., Erni, B., Rak, B., Lengeler, J., Stewart, G. C., Waygood, E. B., & Rappoport, G. (1988b) *Biochimie* **70**, 1743–1748.
- Susi, H., & Byler, D. M. (1986) *Methods Enzymol.* **130**, 290.
- Susi, H., Timasheff, S. N., & Stevens, L. (1967) *J. Biol. Chem.* **242**, 5460–5466.
- Tamm, L. K. (1991) *Biochim. Biophys. Acta* **1071**, 123–148.
- Tamm, L. K., & McConnell, H. M. (1985) *Biophys. J.* **47**, 105–113.
- Tamm, L. K., Tomich, J. M., & Saier, M. H. Jr. (1989) *J. Biol. Chem.* **264**, 2587–2592.
- Tsuboi, M. (1962) *J. Polymer Sci.* **59**, 139–153.
- von Heijne, G. (1988) *Biochim. Biophys. Acta* **947**, 307–333.
- Wolfe, W. L., & Zissis, G. J. (1978) *The Infrared Handbook*, U.S. Government Printing Office.
- Yamada, Y., Chang, Y.-Y., Daniels, G. A., Wu, L.-F., Tomich, J. M., Yamada, M., & Saier, M. H., Jr. (1991) *J. Biol. Chem.* **266**, 17 863–17 871.
- Yoshimura, T., Goto, Y., & Aimoto, S. (1992) *Biochemistry* **31**, 6119–6126.
- Zhang, Y.-P., Lewis, R. N. A. H., Hodges, R. S., & McElhaney, R. N. (1992) *Biochemistry* **31**, 11 572–11 578.